ERDC/EL MP-20-7

US Army Corps
of Engineers®
Engineer Research and
Development Center

Novel Magnetic Nanocarbon and Its Adsorption of Hg and Pb from Water

Kai Guo, Steven L. Larson, John H. Ballard, Zikri Arslan,
Rong Zhang, Yong Ran, Yi Su and Fengxiang X. Han

July 2020

Environmental Laboratory

The U.S. Army Engineer Research and Development Center (ERDC) solves the nation's toughest engineering and environmental challenges. ERDC develops innovative solutions in civil and military engineering, geospatial sciences, water resources, and environmental sciences for the Army, the Department of Defense, civilian agencies, and our nation's public good. Find out more at www.erdc.usace.army.mil.

To search for other technical reports published by ERDC, visit the ERDC online library at http://acwc.sdp.sirsi.net/client/default.

ERDC/EL MP-20-7
July 2020

Novel Magnetic Nanocarbon and Its Adsorption of Hg and Pb from Water

Steven L. Larson and John H. Ballard

Environmental Laboratory
U.S. Army Engineer Research and Development Center
3909 Halls Ferry Road
Vicksburg, MS 39180

Kai Guo, Zikri Arslan, Rong Zhang, and Fengxiang X. Han

Department of Chemistry and Biochemistry
Jackson State University
Jackson, MS 39217

Yong Ran

Chinese Academy of Sciences,
Guangzhou Institute of Geochemistry
Guangzhou, China

Yi Su

School of Science and Computer Engineering
University of Houston — Clear Lake
Houston, TX 77058

Final report

Prepared for U.S. Army Corps of Engineers
Washington, DC 20314

Under Project Number 458170, “Depleted Uranium (DU) Clearance from DoD Ranges”

Abstract

Lead and mercury are two of the most toxic heavy metals in environments. Mesosilicate-templated magnetic nanocarbons with ascorbic acid as carbon precursor were developed through nanocasting processes. The nanocarbon showed effective magnetic separation and the maximum adsorption capacity of 80.6 and 66.3 mg/g for Hg and Pb, respectively. Langmuir model well described adsorption processes of both Hg and Pb from water. Magnetic nanocarbon could be easily separated and incinerated, reducing the volume requiring the disposal. This study indicates that mesosilicate-templated nanocarbons with easy disposal potentials may be good candidates for cleansing Hg and Pb from contaminated water.

Preface

This study was conducted for the U.S. Army Corps of Engineers under Project 458170, titled, "Depleted Uranium (DU) Clearance from DoD Ranges." The Grant Officer's Technical Representative was Mr. John H. Ballard, Office of the Technical Director for Installations and Operational Environments, ERDC-EL-EZT and the Technical Point of Contact was Dr. Steven L. Larson, Environmental Engineering Branch, ERDC-EL-EPE.

The work was performed by the Environmental Engineering Branch of the Environmental Processes Division, U.S. Army Engineer Research and Development Center, Environmental Laboratory (ERDC-EL). At the time of publication of this Miscellaneous Paper, Ms. Brooke Petery was Acting Branch Chief; Dr. Brandon Lafferty was Acting Division Chief; and Dr. Elizabeth Ferguson was the Technical Director for Installations and Operational Environments. The Acting Deputy Director of ERDC-EL was Dr. Justin Berman and the Acting Director was Dr. Jack Davis.

This report documents a collaborative study conducted under the sponsorship of the U.S. Army Futures Command with FY18 Congressional Program Increase Funds in PE 0603728A in the Fiscal Year (FY) 2018 Department of Defense Appropriations Act. Collaborative work was conducted by the U.S. Army Engineer Research and Development Center and Jackson State University via Cooperative Agreement W912HZ-16-2-0021.

The Commander of ERDC was COL Teresa A. Schlosser and the Director was Dr. David W. Pittman.

Novel Magnetic Nanocarbon and Its Adsorption of Hg and Pb from Water

1 Introduction

A significant amount of heavy metals were produced from mining and other anthropogenic activities since industrial revolution (Han et al. 2002, 2003). Heavy metals could come from many industrial sources, for instance, mining, burning of fossil fuels, incineration of wastes, automobile exhausts, smelting processes, sewage sludges as landfill materials, and fertilizers. These contaminants could potentially enter the atmospheric, aquatic, and terrestrial environments (O'Connell et al. 2008). Studies showed that most of major cities in America have been contaminated with Pb due to earlier leaded gasoline consumption and Pb paintings. Lead has contaminated urban soil in the form of fallouts. The lead level in New Orleans urban soil went up to 500 to 1000 mg/kg (Yglesias 2016). Recently, another Pb crisis occurred in Flint, Michigan, since tap water with high level of Pb was used for months (Baum et al. 2016). Pb attacks the brain and central nervous system resulting in children's mental retardation and behavioral disorders and lower IQ (EPA 2000). Therefore, it is essential to develop the effective materials to remove heavy metals such as Pb from water.

Mercury, a trace element, occurs in the earth's crust at $5 \times 10^{-5}\%$. Natural sources and anthropogenic activities produce 10,000 t of mercury each year globally. Naturally occurring Hg is released by degassing the earth's crust, from volcanoes, and evaporation of oceans (Boening 1999). Industrial age anthropogenic mercury production was estimated to be 640,000 t (Han et al. 2002). Mercury has a wide variety of uses in industry,

medicine, dentistry, batteries, science, and military applications. The burning of fossil fuels and medical waste incineration accounts for a majority of all anthropogenic mercury. Chloralkali synthesis (used in electrodes), the wood pulping industry, paints, and electrical equipment industries are major consumption of mercury. However, Hg proves toxic to the central and peripheral nervous systems, digestive and immune systems, lungs, and kidneys. Therefore, both Pb and Hg are in the top list of USEPA.

Due to the high surface area, specific pore volume, and tunable pore size, mesoporous materials have been used for the adsorption of heavy metals and radionuclides (Yang et al. 2009; Guo et al. 2015). Low cost and wide availability also make this class of materials an effective tool for removal of metal contaminants from water. For example, calcium–silicate mesoporous materials synthesized from coal fly ash were shown to be effective for adsorption of Co (Qi et al. 2015). The combination of the characteristics of mesoporous materials, high surface area, specific pore volume, and tunable pore size and the selectivity of organoligands result in a specific sorptive material with high selectivity and efficiency for removal of heavy metals from water. Ethylenediaminetetraacetic acid (EDTA) functionalized mesosilica was confirmed to be effective for the adsorption of Cu and Pb (Ezzeddine et al. 2015).

Mesosilica has also been used as a stable template to synthesize mesoporous carbon with various functional groups such as hydroxyl, carboxyl, and carbonyl groups. Synthesizing this unique porous carbon with ordered hexagonal or cubic structure involved four nanocasting steps: (i) loading the carbonaceous material into the mesosilica, (ii) polymerization of the carbon source, (iii) carbonization of the composite, and (iv) removal of the silica (Baikousi et al. 2013). A number of carbon frames have been produced using sugar(s), including furfuryl alcohol (Lu et al. 2003), acrylonitrile (Lu et al. 2004), styrene (Xia and Mokaya 2004), and divinylbenzene/azobis-(isobutyronitrile) (Yoon et al. 2005). Post-synthesis method was applied to fill carbon source into synthesized mesosilica (Baikousi et al. 2013). Acetylenedicarboxylic acid was chosen as the carbon source, and the composite was applied to the adsorption of Cu, Pb, and Cd. Besides, the co-casting method has been used to prepare magnetic mesoporous carbon, with Santa Barbara Amorphous-15 (*SBA-15*) as a template for the removal of anionic Cr(VI) (Tang et al. 2014).

These contaminants are mostly removed with the polymerized membranes which often require toxic and carcinogenic cross-linker (Barakat 2011; Zhang et al. 2017). The present study proposed the production of sorbents using a self-assembly strategy to synthesize magnetic mesoporous carbon with simultaneous co-casting non-toxic organic carboxylic acid, organosilane source, and iron. Moreover, self-assembly method was employed which was from a mixture of tetraethyl orthosilicate, ascorbic acid, as well as $FeCl_3$ before the calcination (carbonization). The adsorption study was applied to remove Hg and Pb from water. The objectives of this study were to develop novel nanocarbons for removing Pb and Hg from water and to elucidate the mechanism of sorption processes.

2 Materials and Methods

2.1 Materials

Pluronic P123 (EO20PO70EO20, EO = ethylene oxide, PO = propylene oxide), tetraethyl orthosilicate (TEOS), L-ascorbic acid, ethanol, acetone, hydrochloride acid, $HgCl_2$, and $Pb(NO_3)_2$ were purchased from Fisher Science. These reagents were directly used without further purification.

2.2 Synthesis of Mesoporous Nanocarbon

Approximately 2.20 g ascorbic acid was dissolved in 5 mL 0.2 M HCl (aq). About 1.06 g P123 was dissolved in 10 mL ethanol (85.8%) (Wang et al. 2015). Ascorbic acid solution was added dropwise into the ethanol within 30 min. Then, 3 mL tetraethyl orthosilicate (TEOS) was dropped into the mix, which was mixed for another 4 h. The mix was in the hydrothermal treatment for 24 h in the oven. $FeCl_3{\cdot}6H_2O$ (aq) (3.376 g) and 5.4 mL deionized water were added to the mixture and stirred for 4 h. After vacuum filtering, the composite was dried at 60 °C for 5 h. Finally, the composite was calcined in N_2 for 6 h at 900 °C with the increment rate of 5 °C/min.

The silica template of the aforementioned of novel nanocarbon was removed with 1 M NaOH in the ethanol solution ($V_{H2O}/V_{ethanol} = 1{:}1$) shaking at 80 °C with a repeated treatment (each time 30 mL for 30 min) (Baikousi et al. 2013). Finally, the new

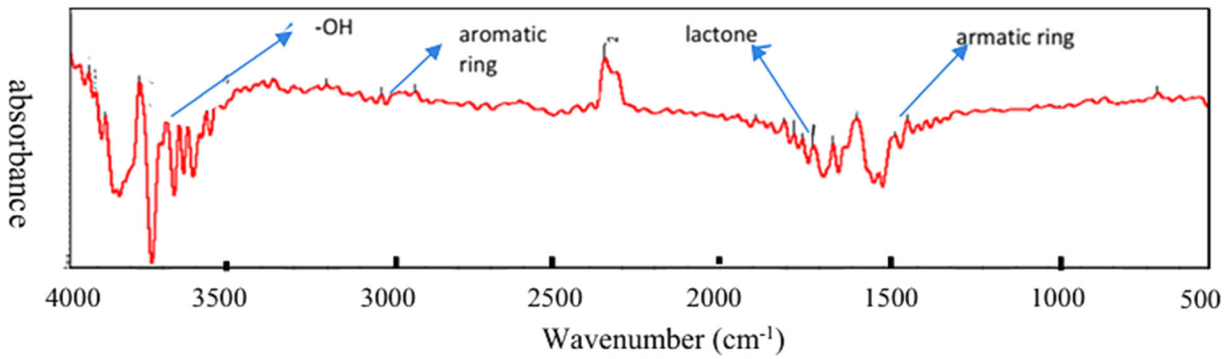

Fig. 1 FTIR spectra of mesosilicate-templated nanocarbons from ascorbic acid as a carbon precursor

nanocarbon was repeatedly washed with deionized water till neutral pH and then was washed with methanol twice in the end. The materials were dried at 80 °C for 6 h.

2.3 Characterization

The Nexus 870 spectrometer was used to get FTIR spectra with 32 scans at 2 cm^{-1} resolution in a frequency range of 400 to 4000 cm^{-1} for determining the functional groups of the materials. Transmission electron microscopy (TEM, JEM-1011) was employed to observe the particles with a resolution of 0.2 nm lattice with a magnification of 50 to 1,000,000 under the accelerating voltage of 40 to 100 kV. Brunauer–Emmett–Teller (BET) surface area and pore size/volume were measured on MicroActive for ASAP 2460 Version 2.01 from Micromeritics.

2.4 Adsorption Study

A Hg adsorption kinetic study was performed on nanocarbons with 3 mg nanocarbons in 10 mL solutions containing 10 mg/L Hg. The mixture was shaken for 5, 10, 20, 30, 60, and 120 min. As showed in the results, 60-min adsorption reached the plateau. For an equilibrium study, 3 mg of ascorbic acid nanocarbon (NC) was added to 10 mL solution in Teflon tube with a series of concentration (0.1, 0.5, 1, 5, 10, 20, and 50 mg/L) of mixture of Hg as $HgCl_2$ and Pb as $Pb(NO_3)_2$. Then, all tubes were shaken in the water bath for 1 h. After centrifuge, the supernatant was filtered and metals were measured with inductively coupled plasma mass spectroscopy (ICP-MS).

Thermodynamic studies were conducted for Hg and Pb. Based on the same adsorption technique as kinetic study and equilibrium study, 10 and 20 mg/L element concentrations were chosen since good adsorption capacity was given under this concentration. Temperatures were set at 15, 30, and 45 °C since this covers the temperature range of mostly possibly seasonally encounted.

Two adsorption models were applied:

Langmuir model:

$$\frac{C_e}{q} = \frac{1}{Qo\,K_L} + \frac{C_e}{Qo} \quad (1)$$

Table 1 Some surface properties of nanocarbons and adsorption parameters of Hg and Pb based on Langmuir model

Surface property	BET surface area (m^2/g)	431	
	Total volume (cm^3/g)	0.84	
	Average pore diameter (nm)	7.77	
Adsorption		Hg	Pb
	Q_o (mg/g)	80.6	66.2
	K_L (L/mg)	2.3	0.062
	R_L	0.005	0.19
	R^2	0.98	0.92

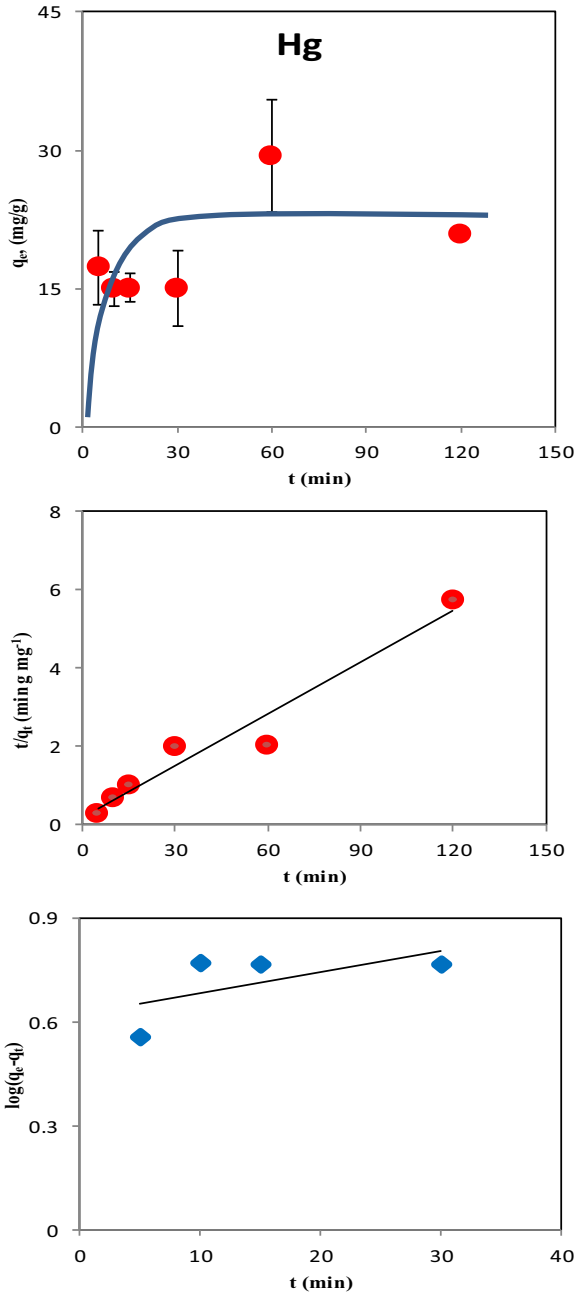

Fig. 2 Kinetic study of Hg adsorption processes on 0.3 g/L nanocarbons at 25 °C and pH = 6~7. Kinetic model (upper), pseudo-second-order (middle), and pseudo-first-order models (bottom) were applied

where C_e denotes the equilibrium concentration, q is the adsorption capacity, K_L (L/mg) relates to the heat of adsorption, and Q_o refers to the maximum adsorption capacity, which is the amount of metal ions at complete monolayer coverage (Yu et al. 2015). Langmuir model assumes that all the adsorption sites have equal adsorbate affinity (Luo et al. 2014). Webi and Chakkravorti (1974) defined the separation factor R_L:

$$R_L = \frac{1}{1 + K_L C_0} \tag{2}$$

Two kinetic models were used to describe adsorption kinetics of metals on nanocarbons:

Pseudo-first model:

$$\ln(q_e - q_t) = \ln q_e - k_1 t \tag{3}$$

where q_e and q_t indicate the amount of adsorbates adsorbed per gram of the adsorbent (mg/g) at equilibrium and any specific time, respectively, and k_1 is the rate constant (per min) (Lagergren 1898).

Pseudo-second model:

$$\frac{t}{q_t} = \frac{1}{k_2 q_e^2} + \frac{t}{q_e} \tag{4}$$

where k_2 is the constant (g/mg/min) (Lagergren 1898). The initial rate h (g/mg/min) is defined as

$$h = k_2 q_e^2 \tag{5}$$

Thermodynamic parameters, Gibbs free energy (ΔG), entropy (ΔS), and enthalpy (ΔH), could be calculated using the following equations (Bazargan-Lari et al. 2014; Meitei and Prasad 2014; Luo et al. 2014; Yargıç et al. 2015):

$$\Delta G = -RT \ln K_C \tag{6}$$

$$K_c = {}^{q_e}/_{C_e} \tag{7}$$

$$\ln K_C = {}^{\Delta S}/_{R} - {}^{\Delta H}/_{RT} \tag{8}$$

(Van't Hoff equation)

where K_C is equilibrium constant and C_e is equilibrium concentration.

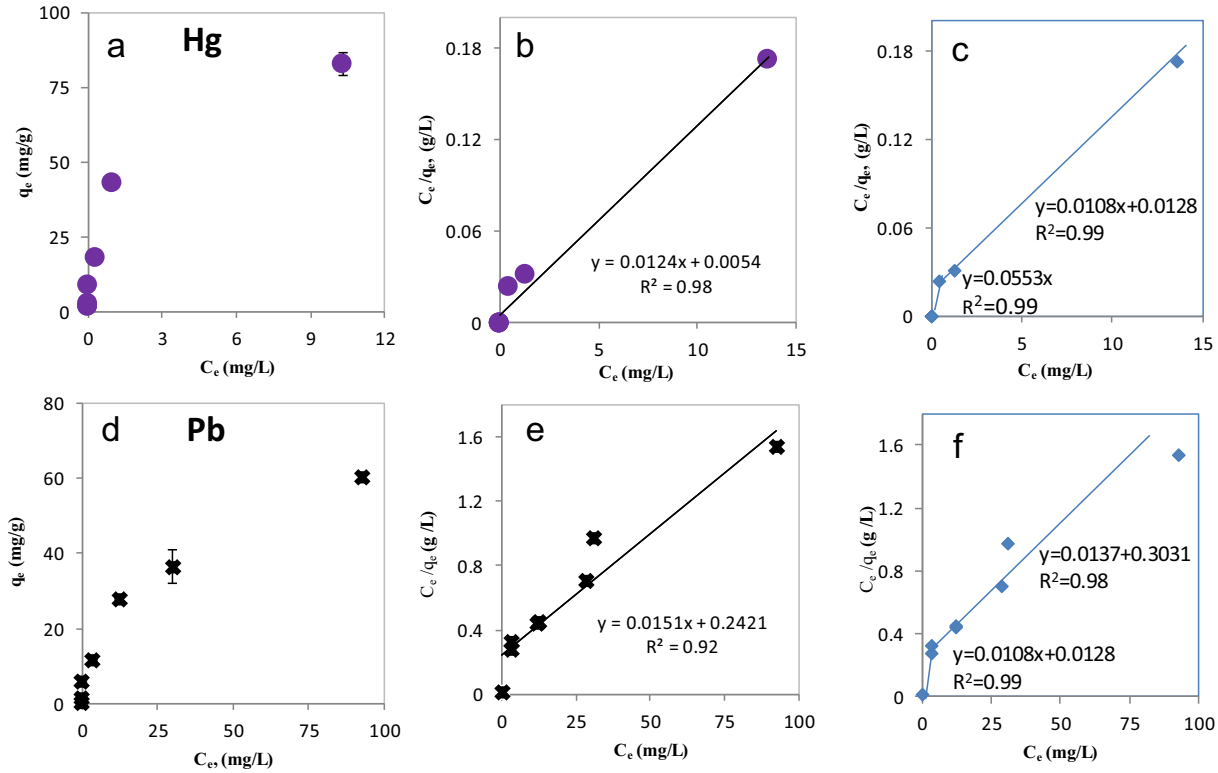

Fig. 3 Adsorption isotherms of Hg (**a**, **b**, **c**,) and Pb (**d**, **e**, **f**) on nanocarbons (0.3 g/L) at 25 °C and pH = 6~7 and Langmuir model applied (Hg, **b**; Pb, **e**) and two linear portions

3 Results and Discussion

3.1 Characterization

Nanocarbons showed functional groups of hydroxyl group in FTIR (Fig. 1). Small peaks at around 3600 cm^{-1} indicated four hydroxyl groups on the structure of nanocarbons. The aromatic structure was shown from a weak peak at 3045 cm^{-1}, which correlated with the medium peak at 1475 cm^{-1} implying C=C in the aromatic structure. Another functional group, lactone, could be seen at 1726.6 cm^{-1}. The TEM image displayed the structure of nanocarbons with a diameter of approximately 5 nm and exhibited more remarkable porosity structure as thinner layer and evenly distributed pores (data not shown). BET showed the pore size around 7.8 nm, which was in the range of mesopores (Lu et al. 2004) and had 431 m^2/g surface area (Table 1).

3.2 Adsorption Kinetic and Adsorption Isotherms

The kinetic data showed that the equilibrium of Hg adsorption reached after 1 h of the adsorption (Fig. 2). The pseudo-second order obtained a better linearity, indicating that the rate-limiting step for the adsorption may depend on chemisorption involving various forces or electron sharing between the adsorbent and Hg (Ho and McKay 1999). The initial adsorption rate from the calculation was 5.23 g/mg/min.

The Langmuir model well fit the adsorption processes of Hg and Pb on nanocarbons (Fig. 3b, e). It showed

Fig. 4 Magnetic effects appeared after a permanent magnet was applied to separate the nanocarbons from water solution

the adsorption of Hg with a maximum adsorption capacity of 80 mg/g at equilibrium concentrations of 7 mg/L. Likewise, adsorption of Pb showed the maximum adsorption capacity of 66 mg/g at equilibrium concentration of around 30 mg/L, indicating the less efficiency of Pb adsorption than Hg. R_L was 0.0054 and 0.195 for Hg and Pb, respectively, implying the favorable nature in both adsorption scenarios. Since mesoporous characteristics, adsorption isotherms of both Pb and Hg may be better described with two-section linear equations (Fig. 3c, f) with an initial physical and later possible chemical adsorption and diffuse into inside the pores.

After the sorption processes, a permanent magnet was applied to separate nanocarbon particles from water solution (Fig. 4). The sorbent was observed to be attracted by the magnet so that the sorbent was separated from the solution successfully. To avoid the second-time contamination after the sorption process, separation with magnetism has been an effective separation approach. Regardless of the functionalization, magnetic nanoparticle has higher aggregation property. Norouzian and Lakouraj (2015) employed vibrating sample magnetometer (VSM) to measure the saturation magnetization for Fe_3O_4@PANI-AmAzoTCA [4] (magnetic polymerized thiacalix) and Fe_3O_4. The grafted Fe_3O_4 has 50.67 emu/g compared with Fe_3O_4 of 54 emu/g. Therefore, the magnetic composite performed well for the separation.

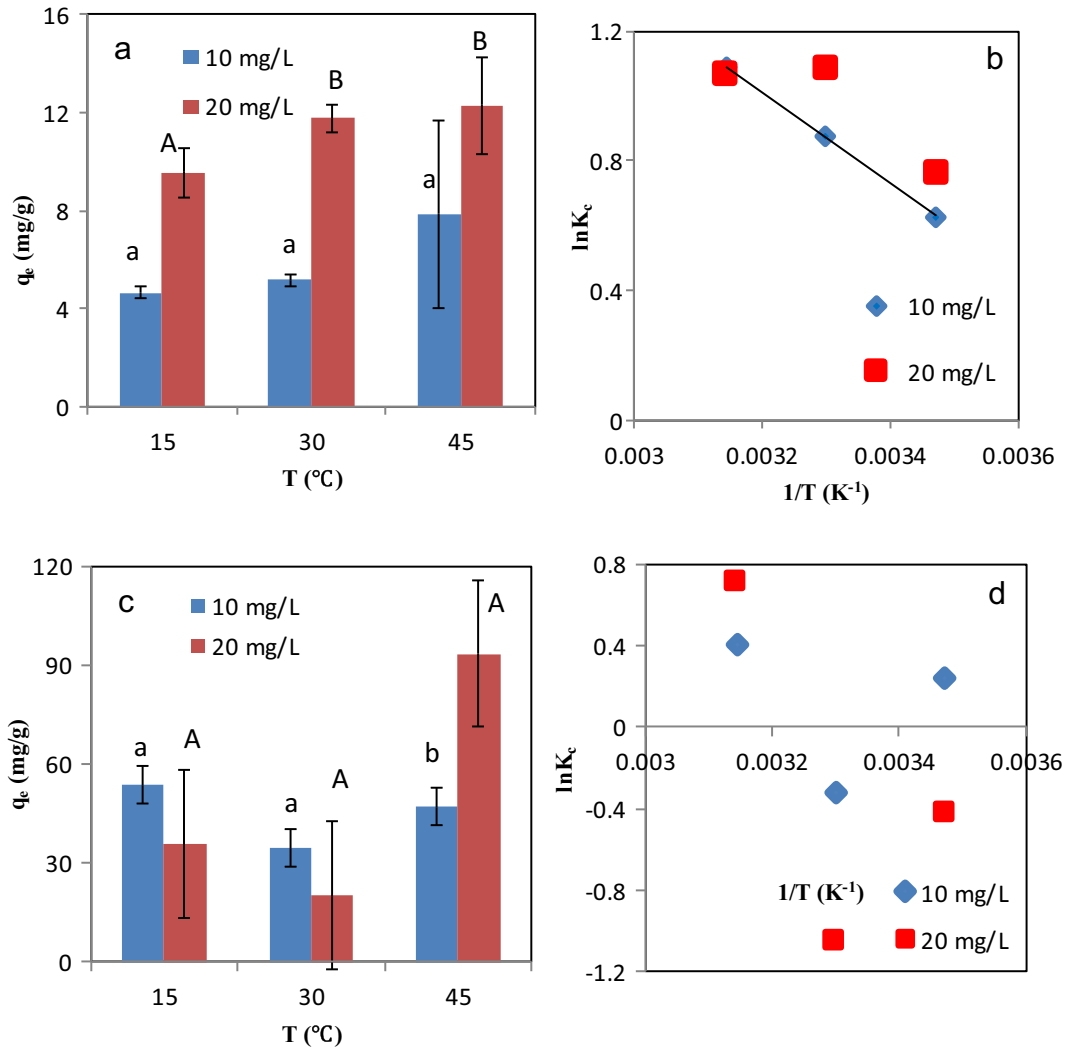

Fig. 5 Thermodynamic study of adsorption processes of Hg (**a**) and Pb (**c**) with Van't Hoff model applied, Hg (**b**) and Pb (**d**). For **a** and **c**, the same letter for temperature treatments with each initial concentration indicated no significant difference at $p = 0.05$

Table 2 Thermodynamic parameters of Hg and Pb adsorption processes on nanocarbons at 10 and 20 mg/L concentration at pH 6–7

Metals	Temperature (°C)	Initial Concentrations of metals									
		10 mg/L					20 mg/L				
		ΔG (kJ/mol)	$\ln K_C$	ΔH (kJ/mol)	ΔS (J/mol/K)	R^2	ΔG (kJ/mol)	$\ln K_C$ (kJ/mol)	ΔH (J/mol/K)	ΔS	R^2
Hg	15	− 1.51	0.63			1	− 1.83	0.76			0.74
	30	− 2.1	0.88	11.6	45.6		− 2.73	1.09	7.93	34.3	
	45	− 2.6	1.09				− 2.83	1.07			
Pb	15	− 0.57	0.24			0.037	1.01	− 0.42			0.38
	30	0.8	− 0.32				2.64	− 1.05			
	45	− 1.07	0.4				− 1.88	0.71			

3.3 Adsorption Thermodynamics

For thermodynamic study, two initial concentrations of Hg and Pb (10 and 20 mg/L) and three different temperatures (15, 30, and 45 °C) were applied (Fig. 5, Table 2). As the temperature increased, the adsorption capacity of Hg enhanced for both initial concentrations (Table 2). Negative ΔG indicates that the adsorption processes were the favorable and spontaneous process. Since ΔG is small for Pb, there was some fluctuation in ΔG values due to some experimental condition control. The positive ΔH indicated that the adsorption was endothermic with possible chemisorption mechanism. Besides, positive ΔS implied the increasing randomness at the sorbent–sorbate surface. When Hg concentration increased to 20 mg/L, the linearity started to decline, as the result of the saturation of the adsorbent. The ΔG values indicated the spontaneity of the adsorption. Yet there was a decrease for both ΔH and ΔS. Since the increase in the temperature, the vibration of the functional groups increased, which was attributed to the unstable binding of Hg on the adsorbent. Nevertheless, the linearity of Pb was not good in terms of Van't Hoff equation. For Pb adsorption, ΔG was fluctuated around zero as the temperature increased, whereas the Langmuir model gave a good isotherm adsorption at 25 °C. This may indicate the possible role of physicosorption mechanism, which is the inclusion of Pb in the pores of the adsorbent (Zhao et al. 2015).

It was reported that the carbon nanotubes and Mn-immobilized silica NP exhibited a good adsorption capacity of Hg in the neutral environment (Table 3). The present study indicated that the good adsorption capacity could be achieved in removing both Pb and Hg from water with the nanocasting nanocarbons, which showed a promise for treatment of industrial wastewater.

4 Conclusion

Novel nanocarbons were synthesized with the template of mesosilica through nanocasting processes. Experimental results confirmed that the nanocarbons were efficient in removing Hg and Pb from water. Magnetic

Table 3 Comparison of adsorption capacity of Hg and Pb on different adsorbents

Adsorbents	Metals	Optimal pH	Maximum adsorption capacity (mg/g)	References
MnO_2-coated carbon	Hg	5–6	58.8	Moghaddam and Pakizeh (2015)
Si/Al-PAEA=SA@MnNP		6	290	Arshadi (2015)
Nanocarbon		6–7	85	This study
Fe_3O_4/SiO_2 nanocomposite	Pb	4	17.6	Mahdavi et al. (2013)
Oxidized carbon nanotube		7–10	2.05	Xu et al. (2008)
Nanocarbon		6–7	66.2	This study

nanocarbon could be easily separated from solution and ready to be incinerated, reducing the volume requiring disposal. This study indicates that mesosilicate-templated nanocarbons with easy disposal potentials may be good candidates for cleansing Hg and Pb from contaminated water.

Acknowledgements This study was supported by the US Army Environmental Quality Technology (EQT) Program, the US Army Engineer Research and Development Center (Cooperative Agreement W912HZ-16-2-0021), the US Nuclear Regulatory Commission (NRC-HQ-84-15-G-0042 and NRC-HQ-12-G-38-0038), and the US Department of Commerce (NOAA) (NA11SEC4810001-003499).

References

Arshadi, M. (2015). Manganese chloride nanoparticles: a practical adsorbent for the sequestration of Hg(II) ions from aqueous solution. *Chemical Engineering Journal, 259*, 170–182.

Baikousi, M., Daikopoulos, C., Georgiou, Y., et al. (2013). Novel ordered mesoporous carbon with innate functionalities and superior heavy metal uptake. *Journal of Physical Chemistry C, 117*, 16961–16971.

Barakat, M. A. (2011). New trends in removing heavy metals from industrial wastewater. *Arabian Journal of Chemistry, 4*, 361–377.

Baum, R., Bartram, J., & Hrudey, S. (2016). The flint water crisis confirms that U.S. drinking water needs improved risk management. *Environmental Science & Technology, 50*, 5436–5437.

Bazargan-Lari, R., Zafarani, H. R., Bahrololoom, M. E., & Nemati, A. (2014). Removal of Cu(II) ions from aqueous solutions by low-cost natural hydroxyapatite/chitosan composite: equilibrium, kinetic and thermodynamic studies. *Journal of the Taiwan Institute of Chemical Engineers, 45*, 1642–1648.

Boening, D. W. (1999). Ecological effects, transport, and fate of mercury: a general review. *Chemosphere, 40*, 1335–1351.

Guo, K., Han, F. X., Arslan, Z., et al. (2015). Adsorption of Cs from water on surface modified MCM-41 mesosilicate. *Water Air Soil Pollution, 226*, 288–297.

EPA (2000) America's Children and the Environment—A First View of Available Measures.

Ezzeddine, Z., Batonneau-Gener, I., Pouilloux, Y., et al. (2015). Divalent heavy metals adsorption onto different types of EDTA-modified mesoporous materials: effectiveness and complexation rate. *Microporous and Mesoporous Materials, 212*, 125–136.

Han, F. X., Banin, A., Su, Y., et al. (2002). Industrial age anthropogenic inputs of heavy metals into the pedosphere. *Naturwissenschaften, 89*, 497–504.

Han, F. X., Su, Y., Monts, D. L., et al. (2003). Assessment of global industrial-age anthropogenic arsenic contamination. *Naturwissenschaften, 90*, 395–401.

Ho, Y., & McKay, G. (1999). Pseudo-second order model for sorption processes. *Process Biochemistry, 34*, 451–465.

Lagergren, S. (1898). About the theory of so-called adsorption of soluble substances. *K Sven Vetenskapsakademiens Handl, 24*, 1898.

Lu, A., Kiefer, A., Schmidt, W., & Ferdi, S. (2004). Synthesis of polyacrylonitrile-based ordered mesoporous carbon with tunable pore structures. *Chermistry Mater, 16*, 100–103.

Lu, A. H., Schmidt, W., Spliethoff, B. & Schuth, F. (2003). Synthesis of ordered mesoporous carbon with bimodal pore system and high pore volume. *Advanced Materials, 15*, 1602–1606.

Luo, S., Xu, X., Zhou, G., et al. (2014). Amino siloxane oligomer-linked graphene oxide as an efficient adsorbent for removal of Pb(II) from wastewater. *Journal of Hazardous Materials, 274*, 145–155.

Mahdavi, M., Bin, A. M., Haron, M. J., et al. (2013). Fabrication and characterization of SiO2/(3-aminopropyl)triethoxysilane-coated magnetite nanoparticles for lead(II) removal from aqueous solution. *Journal of Inorganic and Organometallic Polymers and Materials, 23*, 599–607.

Meitei, M. D., & Prasad, M. N. V. (2014). Adsorption of Cu(II), Mn(II) and Zn(II) by Spirodela polyrhiza (L.) Schleiden: equilibrium, kinetic and thermodynamic studies. *Ecological Engineering, 71*, 308–317.

Moghaddam, H. K., & Pakizeh, M. (2015). Experimental study on mercury ions removal from aqueous solution by MnO_2/CNTs nanocomposite adsorbent. *Journal of Industrial and Engineering Chemistry, 21*, 221–229.

Norouzian R, Lakouraj MM (2015) Preparation and heavy metal ion adsorption behavior of novel supermagnetic nanocomposite based on thiacalix [4] arene and polyaniline: conductivity, isotherm and kinetic study. 203:135–148.

O'Connell, D. W., Birkinshaw, C., & O'Dwyer, T. F. (2008). Heavy metal adsorbents prepared from the modification of cellulose: a review. *Bioresource Technology, 99*, 6709–6724.

Qi, G., Lei, X., Li, L., et al. (2015). Preparation and evaluation of a mesoporous calcium-silicate material (MCSM) from coal fly ash for removal of Co(II) from wastewater. *Chemical Engineering Journal, 279*, 777–787.

Tang, L., Yang, G.-D., Zeng, G.-M., et al. (2014). Synergistic effect of iron doped ordered mesoporous carbon on adsorption-coupled reduction of hexavalent chromium and the relative mechanism study. *Chemical Engineering Journal, 239*, 114–122.

Wang, F., Liang, L., Shi, L., et al. (2015). CO2 assisted synthesis of highly dispersed Co_3O_4 nanoparticles on mesoporous carbon for lithium ion battery. *Journal of Alloys and Compounds, 633*, 65–70.

Webi, T. W., & Chakravort, R. K. (1974). Pore and solid diffusion models for fixed-bed adsorbers. *AICHE Journal, 20*, 228–238.

Xia, Y., & Mokaya, R. (2004). Synthesis of ordered mesoporous carbon and nitrogen-doped carbon materials with graphitic pore walls via a simple chemical vapor deposition method. *Advanced Materials, 16*, 1553–1558.

Xu, D., Tan, X., Chen, C., & Wang, X. (2008). Removal of Pb(II) from aqueous solution by oxidized multiwalled carbon nanotubes. *Journal of Hazardous Materials, 154*, 407–416.

Yang Z, Lu Y, Yang Z (2009) Mesoporous materials: tunable structure, morphology and composition. *Chemical Communications 2270*.

Yargıç, A. Ş., Şahin, R. Z. Y., Özbay, N., & Önal, E. (2015). Assessment of toxic copper(II) biosorption from aqueous

solution by chemically-treated tomato waste. *Journal of Cleaner Production, 88*, 152–159.

Yglesias M (2016) It's not just flint—every major American city has hazardous amounts of lead hurting kids. In: Vox. http://www.vox.com/2016/1/19/10790534/lead-soil. Accessed 19 Jan 2016.

Yoon, S. B., Kim, J. Y., Yu, J.-S., et al. (2005). Fabrication and characterization of mesostructured silica, HUM-1, and its ordered mesoporous carbon replica. *Industrial and Engineering Chemistry Research, 44*, 4316–4322.

Yu, S., Wang, X., Tan, X., & Wang, X. (2015). Sorption of radionuclides from aqueous systems onto graphene oxide-based materials: a review. *Inorganic Chemistry Frontiers, 2*, 593–612.

Zhang, P., Gong, J.-L., Zeng, G.-M., et al. (2017). Cross-linking to prepare composite graphene oxide-framework membranes with high-flux for dyes and heavy metal ions removal. *Chemical Engineering Journal*. https://doi.org/10.1016/j.cej.2017.04.068.

Zhao, F., Repo, E., Yin, D., et al. (2015). EDTA-cross-linked β-cyclodextrin: an environmentally friendly bifunctional adsorbent for simultaneous adsorption of metals and cationic dyes. *Environmental Science & Technology, 49*, 10570–10580.

REPORT DOCUMENTATION PAGE

Form Approved
OMB No. 0704-0188

1. REPORT DATE (DD-MM-YYYY)	2. REPORT TYPE	3. DATES COVERED (From - To)
July 2020	Final	

4. TITLE AND SUBTITLE

Novel Magnetic Nanocarbon and Its Adsorption of Hg and Pb from Water

5a. CONTRACT NUMBER

5b. GRANT NUMBER

5c. PROGRAM ELEMENT NUMBER
633728 03F

6. AUTHOR(S)

Kai Guo, Steven L. Larson, John H. Ballard, Zikri Arslan, Rong Zhang, Yong Ran, Yi Su, and Fengxiang X. Han

5d. PROJECT NUMBER
458170

5e. TASK NUMBER
5

5f. WORK UNIT NUMBER

7. PERFORMING ORGANIZATION NAME(S) AND ADDRESS(ES)
U.S. Army Engineer Research and Development Center
Environmental Laboratory
3909 Halls Ferry Road
Vicksburg, MS 39180

8. PERFORMING ORGANIZATION REPORT NUMBER

ERDC/EL MP-20-7

9. SPONSORING / MONITORING AGENCY NAME(S) AND ADDRESS(ES)
Budget and Programs Div
Department of the Army USACE
441 G Street NW
Washington, DC 20314

10. SPONSOR/MONITOR'S ACRONYM(S)

USACE

11. SPONSOR/MONITOR'S REPORT NUMBER(S)

12. DISTRIBUTION / AVAILABILITY STATEMENT
Approved for public release; distribution is unlimited.

13. SUPPLEMENTARY NOTES
Originally published in the Journal of Water Air Soil Pollution, March 2018.
Collaborative work was conducted by the U.S. Army ERDC and Jackson State University via Cooperative Agreement W912HZ-16-2-002.

14. ABSTRACT

Lead and mercury are two of the most toxic heavy metals in environments. Mesosilicate-templated magnetic nanocarbons with ascorbic acid as carbon precursor were developed through nanocasting processes. The nanocarbon showed effective magnetic separation and the maximum adsorption capacity of 80.6 and 66.3 mg/g for Hg and Pb, respectively. Langmuir model well described adsorption processes of both Hg and Pb from water. Magnetic nanocarbon could be easily separated and incinerated, reducing the volume requiring the disposal. This study indicates that mesosilicate-templated nanocarbons with easy disposal potentials may be good candidates for cleansing Hg and Pb from contaminated water.

15. SUBJECT TERMS

Adsorption, Mesoporous, Nanocarbon, Silicate, Radionuclide, Heavy metals

16. SECURITY CLASSIFICATION OF:			17. LIMITATION OF ABSTRACT	18. NUMBER OF PAGES	19a. NAME OF RESPONSIBLE PERSON
a. REPORT	b. ABSTRACT	c. THIS PAGE			19b. TELEPHONE NUMBER (include area code)
Unclassified	Unclassified	Unclassified	SAR	13	